Structure-Dependent Electronic Nature of Star-Shaped Oligothiophenes, Probed by Ensemble and Single-Molecule Spectroscopy

ARTICLE *in* CHEMISTRY - A EUROPEAN JOURNAL · JULY 2013

Impact Factor: 5.73 · DOI: 10.1002/chem.201300313 · Source: PubMed

7 AUTHORS, INCLUDING:

Masayoshi Takase
Tokyo Metropolitan University
50 PUBLICATIONS **844** CITATIONS
SEE PROFILE

Iyoda Masahiko
Tokyo Metropolitan Institute
364 PUBLICATIONS **4,842** CITATIONS
SEE PROFILE

Dongho Kim
Yonsei University
499 PUBLICATIONS **13,497** CITATIONS
SEE PROFILE

CHEMISTRY
A EUROPEAN JOURNAL

FULL PAPER

DOI: 10.1002/chem.201300313

Structure-Dependent Electronic Nature of Star-Shaped Oligothiophenes, Probed by Ensemble and Single-Molecule Spectroscopy

Heejae Chung,[a] Tomoyuki Narita,[b] Jaesung Yang,[a] Pyosang Kim,[a] Masayoshi Takase,[b] Masahiko Iyoda,*[b] and Dongho Kim*[a]

Abstract: We have investigated the photophysical properties of star-shaped oligothiophenes with three terthiophene arms (*meta* to each other, **S3**) or six terthiophene arms (*ortho*-, *meta*-, and *para*-arranged, **S6**) connected to an ethynylbenzene core to elucidate the relationship between their molecular structure and electronic properties by using a combination of ensemble and single-molecule spectroscopic techniques. We postulate two different conformations for molecules **S3** and **S6** on the basis of the X-ray structure of hexakis(5-hexyl-2-thienlyethynyl)benzene and suggest the coexistence of these conformers by using spectroscopic methods. From the steady-state spectroscopic data of compound **S6**, we show that the exciton is delocalized over the core structure, but that the *meta*-linkage in compound **S3** prevents the electronic communication between the arms. However, in single-molecule spectroscopic measurements, we observed that some molecules of compound **S3** showed long fluorescence lifetimes (about 1.4 ns) in the fluorescence-intensity trajectories, which indicated that π electrons were delocalized along the *meta* linker. Based on these observations, we suggest that the delocalized exciton is intensely sensitive towards the dihedral angle between the core and the adjacent thiophene ring, as well as to the substituted position of the terthiophene arms. Our results highlight that the fluorescence lifetimes of compounds **S3** and **S6** are strongly correlated with the spatial location of their excitons, which is mainly affected by their conformation, that is, whether the innermost thiophene rings are facing each other or not. More interestingly, we observed that the difference between the degrees of ring-torsional flexibility of compounds **S3** and **S6** results in their sharply contrasting fluorescence properties, such as a change in fluorescence intensity as a function of temperature.

Keywords: delocalization · electronic structure · oligothiophenes · single-molecule studies · time-resolved spectroscopy

Introduction

Over the past few years, organic materials have been the subject of intensive research for a range of optoelectronic applications, such as organic light-emitting diodes (OLEDs), light-emitting field-effect transistors (FETs), and organic photovoltaic (OPV) devices.[1–3] In particular, conjugated polymers have recently become one of the most-widely studied materials for use as electronic/photonic devices. Conjugated polymers allow the use of simple and fast device-manufacturing processes because they are soluble and can be deposited from solution by using inexpensive processes, such as spin-coating, spraying, and ink-jet printing.[4] However, it is difficult to control the polydispersity, molecular weight, and backbone defects in conjugated polymers in a reproducible manner.[5] To circumvent these drawbacks, several other geometries of small molecules, such as linear, cyclic, and star-shaped oligomers and low-generation dendrimers, have been studied despite their lower solubility compared to polymers.

Conjugated oligomers have the advantage that the relationships between their structure and properties are relatively well-understood in comparison with polymers, as well as the fact that their materials are monodisperse.[5,6] Whereas the majority of research activities have been focused on straight-chain oligomers, much attention has recently been paid to branched molecules.[6–9] Branched molecules, known as star-shaped molecules and dendrimers, offer high tunability of their electronic structure by controlling the size or functional groups on the molecules, which significantly affect their carrier mobility. Through tailoring functional groups in the core and the arm, the photophysical and photovoltaic parameters of star-shaped molecules and dendrimers can be tuned for improving the performance of the devices.[10–15]

[a] H. Chung, Dr. J. Yang, P. Kim, Prof. D. Kim
Department of Chemistry and Spectroscopy Laboratory for Functional π-Electronic Systems, Yonsei University
262 Seongsanno Seodaemun-gu, Seoul 120-749 (Korea)
Fax: (+82) 2-2123-2434
E-mail: dongho@yonsei.ac.kr

[b] Dr. T. Narita, Dr. M. Takase, Prof. M. Iyoda
Department of Chemistry, Graduate School of Science and Engineering, Tokyo Metropolitan University
Hachioji, Tokyo 192-0397 (Japan)
Fax: (+81) 42-677-2525
E-mail: iyoda@tmu.ac.jp

Supporting information for this article is available on the WWW under http://dx.doi.org/10.1002/chem.201300313.

The thiophene repeating unit has been extensively utilized as a fundamental building block for numerous organic optoelectronic systems.[16–21] Oligothiophenes and thiophene derivatives have found a unique place among several organic chromophores that have been employed to synthesize dendritic structures, owing to their high stability, ease of processing, self-assembly properties, charge transport, and applications in organic photonics and electronics.[6]

Herein, we have employed two different star-shaped oligothiophene molecules to determine the effect of different substituted positions on their interchromophore interactions:[22] One oligothiophene is a *meta*-arranged trimer (**S3**), with three conjugated thiophene arms and a 1,3,5-triethynylbenzene core, whereas the other oligothiophene is an *ortho*-, *meta*-, and *para*-arranged hexamer (**S6**), with six arms and a hexaethynylbenzene core (Scheme 1). To enhance their solution-processability, *n*-butyl groups were introduced onto the two outmost thiophene rings on each arm.[21,22] In a previous study, their synthesis and fundamental optical properties, such as absorption and emission, have been reported.[21] In this work, we investigated the photoelectronic properties of star-shaped compounds **S3** and **S6**, with a focus on their π-conjugation length and their molecular rigidity.

We measured temperature-dependent absorption and fluorescence spectra to explore the differences between their photophysical properties with conformation changes of compounds **S3** and **S6**. We found that the fluorescence spectra of compounds **S3** and **S6** exhibited opposite trends in intensity change with increasing temperature: As the temperature increased, the fluorescence intensity of compound **S3** increased, whereas that of compound **S6** decreased.

Single-molecular spectroscopic techniques have been useful for providing invaluable information on individual constituent chromophores and their interactions in multichromophoric systems. In this regard, we have utilized single-molecule fluorescence microscopy (SMFS) to observe the differences between the intramolecular interactions in compounds **S3** and **S6**, in relation to their substitution pattern, as well as the unique contribution of each conformer of compounds **S3** and **S6**. By using single-molecule experiments, we found that, whereas compound **S3** showed a three-step intensity level, compound **S6** exhibited one- or two-step intensity levels, from which detailed information on the spatial location of the excitons that were formed upon photoexcitation, which was dependent on the molecular geometry, could be obtained. All of these data indicate that there is a strong correlation between the molecular

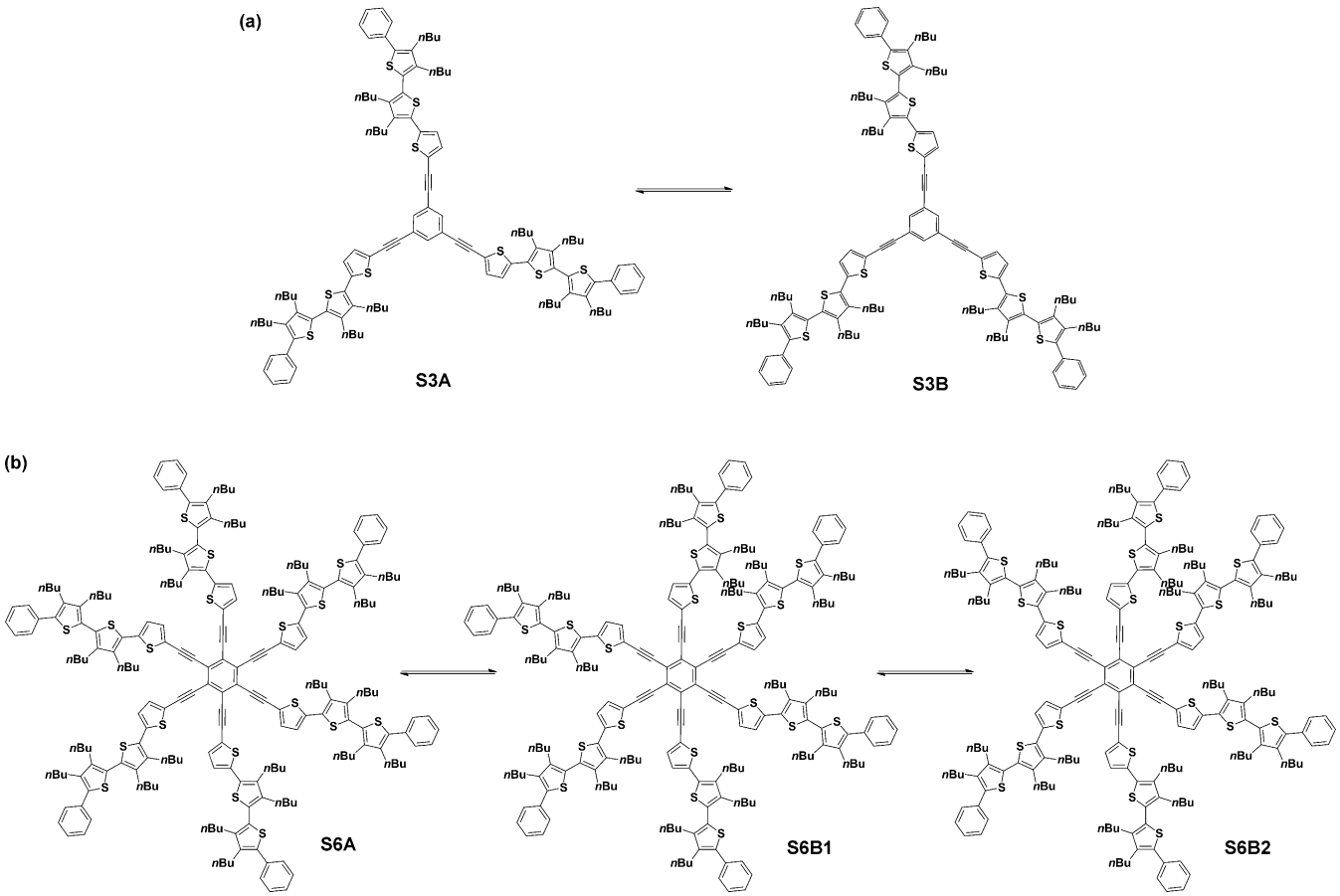

Scheme 1. Molecular structures of a) compound **S3** and b) compound **S6**. In structures **S3A** and **S6A**, the innermost thiophene rings are arranged in a counter-clockwise direction, whereas, in structures **S3B** and **S6B**, one or two of the innermost thiophene rings are flipped over.

structures of compounds **S3** and **S6** and their electronic nature.

Results and Discussion

Molecular structures and ensemble measurements: We prepared star-shaped oligothiophenes with three *meta*-arranged terthiophene arms (**S3**) and six *ortho*-, *meta*-, and *para*-arranged arms (**S6**) connected to central D_{3h}-symmetric triethynylbenzene and D_{6h}-symmetric hexaethynylbenzene cores, respectively (Scheme 1). To improve the solubility of compounds **S3** and **S6**, four butyl groups were introduced onto the two outmost thiophene rings in each terthiophene arm.[21] Based on the X-ray structures of hexakis(5-hexyl-2-thienylethynly)benzene, in which two thiophene rings are flipped over (see the Supporting Information, Table S1), together with hexabutylthio-1,3,5-tris(tetrathiafulvalenly)benzene,[24] each probable conformer of compounds **S3** and **S6** is taken into account (Scheme 1). It has been reported that the alkyl substituents in the directly linked oligothiophene systems lead to twisting of the molecular backbone.[25,26] Furthermore, the average distance between the neighboring terthiophene arms in compound **S6** is so short (about 10 Å) that the butyl groups cannot adopt a geometry that minimizes steric congestion. The difference between the molecular geometries of those conformers is as expected, based on the spatial location of the butyl groups. In this regard, we calculated the conformational stability of the optimized ground-state geometries of compounds **S3** and **S6** with butyl groups on two outmost thiophene rings at the PM6 level of theory (see the Supporting Information, Figure S1). Herein, we assign the innermost thiophene ring, which can point clockwise or anticlockwise, as P for plus and M for minus, respectively. In this way, for compound **S3**, there are two conformers that have a diastereomeric relationship: **S3A** (MMM) and **S3B** (MMP). However, in the case of compound **S6**, the total number of probable conformers in diasteromeric relationships is eight and the situation is much more complex than that for compound **S3**. In both systems **S3** and **S6**, structures **S3A** (MMM) and **S6A** (MMMMMM), in which the innermost thiophene rings are arranged in either all-clockwise or all-counter-clockwise directions, are the most stable. However, the inversion of one thiophene ring readily takes place in compound **S3** because of its molecular flexibility and conformational stability. In compound **S6**, although steric congestion prohibits the rotational motion of the thiophene ring, the coexistence of conformers is quite plausible because structures **S6B1** (MMMMMP) and **S6B2** (MMMMPP) are only +0.75 and +0.60 kcal mol^{-1} higher in energy than structure **S6A**, respectively. However, the remainder of these structures exhibit states that are about 4 kcal mol^{-1} higher in energy than structure **S6A**, which indicates that the diastereomeric forms of compound **S6**, except for structures **S6A**, **S6B1**, and **S6B2**, have extremely low probability densities. In this regard, other diastereomeric forms, that is, the MMMPMP, MMPMMP, MMMPPP, MMPPMP, and MPMPMP forms, are not taken into account because their level of contribution to the photophysical properties of compound **S6** is negligible.

The optimized geometries of compound **S3** have bowl-shape structures and the terthiophene arms are not in the same plane as the phenyl core. In the optimized geometries of compound **S6**, the average six dihedral angles between the core and each of innermost thiophene rings (about 29.4°) are larger than those in compound **S3** (about 12.8°), owing to steric hindrance between the neighboring terthiophene arms. Furthermore, in compound **S6**, the optimized structures exhibit distinctive structural differences, in particular in terms of the dihedral angle between the core and each of innermost thiophene rings. Because the innermost thiophene ring of the terthiophene arm flips over such that two sulfur atoms of neighboring innermost thiophene rings face each other, these thiophene rings and their *para*-positioned counterparts form relatively small dihedral angles (<25°) with respect to the plane of the benzene core in compound **S6** (see the Supporting Information, Figure S1). The vertical transition energies were calculated by using time-dependent density functional theory (TD-DFT) with the B3LYP hybrid functional and the 6-31G (d,p) basis set, with optimized geometries without butyl groups (see the Supporting Information, Figure S2). The simulated absorption spectra agree well with the experimental data.

Previous studies on oligothiophenes and other conjugated molecules have verified that a twisted backbone has a disruptive impact on the π-electron delocalization.[26,27] As discussed above, compound **S6** has large dihedral angles between the core and the attached thiophene rings. However, as shown in Figure 1a, the maximum peaks in the absorption and fluorescence spectra of compound **S6** are shifted to longer wavelength compared to those of compound **S3**. A gradual red-shift in the absorption and fluorescence spectra with increasing number of thiophene units has been reported for various linear oligothiophene systems. The absorption peaks of star-shaped compounds **S3** and **S6** appear in a similar spectroscopic region to those of directly linked linear tri-

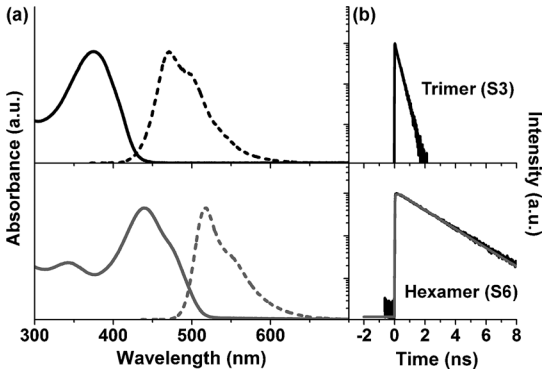

Figure 1. a) Steady-state absorption (solid lines) and fluorescence (dotted lines) spectra of compounds **S3** (top) and **S6** in toluene (bottom). b) Fluorescence-decay profiles of compound **S3** (black line) after excitation at 400 nm and compound **S6** (gray line) after excitation at 450 nm in toluene.

meric and hexameric oligothiophenes, respectively.[28] These results corroborate the presence of electronic communication between the arms for compound **S6**. It has been reported that a *para* linker is the most effective in elongating the π-conjugation pathway, whereas a *meta* linker is not as effective in extending the π-conjugation length.[29] In this regard, we can conceive that the absence of interchromophoric interactions between the arms in compound **S3** is attributed to its *meta*-arranged structure. On the other hand, *ortho*-, *meta*-, and *para*-arranged compound **S6** allows electronic communication between the *para*-positioned arms and the π conjugation is elongated through the *para* linker. The molecular orbital (MO) diagrams also verify the presence of electronic communication between the *para*-positioned terthiophene arms of compound **S6** in the ground state, whereas the MO shapes of compound **S3** show that the electron density is localized on each terthiophene arm (see the Supporting Information, Figure S3).

Recent experimental investigations on oligothiophenes have demonstrated the importance of intersystem crossing (ISC) processes as a nonradiative decay route of the singlet excitations. A decrease in the ISC rate contributes to an increase in the fluorescence quantum yield and fluorescence lifetime with increasing oligothiophene chain-length.[28,30] In accordance with these above results, the quantum yield of compound **S6** (0.36) is larger than that of compound **S3** (0.22) and the observed fluorescence lifetime of compound **S6** (1.9 ns) is about one order of magnitude longer than that of compound **S3** (280 ps) in toluene (Figure 1b). All of these results can be also understood by an elongation of the π-conjugation length along the *para*-positioned arms in compound **S6**. The corresponding absorption and fluorescence properties of compounds **S3** and **S6** are summarized in Table 1.

Table 1. Photophysical properties of compounds **S3** and **S6**.

	Stokes shift [cm^{-1}]	Φ_F[a]	τ_F[b]	k_r [$\times 10^8\ s^{-1}$]	k_{nr} [$\times 10^8\ s^{-1}$]
S3	5435	0.22	280 ps	7.86	27.87
S6	1844	0.36	1.9 ns	1.89	3.36

[a] Φ_F indicates the relative fluorescence quantum yield, referenced to rhodamine 6G in EtOH (0.95), at an excitation wavelength of 480 nm. [b] τ_F is the fluorescence lifetime, as measured by photoexcitation at 400 nm for compound **S3** and 450 nm for compound **S6**.

Thermochromic properties of compounds S3 and S6: To determine the relationship between the photophysical properties of compounds **S3** and **S6** and their conformational changes, we measured their steady-state absorption, fluorescence spectra, and fluorescence-decay profiles by using the time-correlated single-photon-counting (TCSPC) technique within the temperature range 77–297 K (Figure 2). We found that each terthiophene arm separately emitted photons in compound **S3**, but electronically interacting *para*-arranged arms emitted fluorescence as a single chromophore in compound **S6**. To simplify these systems, we have categorized the conformations of compounds **S3** and **S6** into two and three groups, respectively, on the basis of the arrangement of the innermost thiophene rings. However, it should be assumed that the various conformations of compounds **S3** and **S6** coexist because of the freedom in all of the dihedral angles between the thiophene moieties.

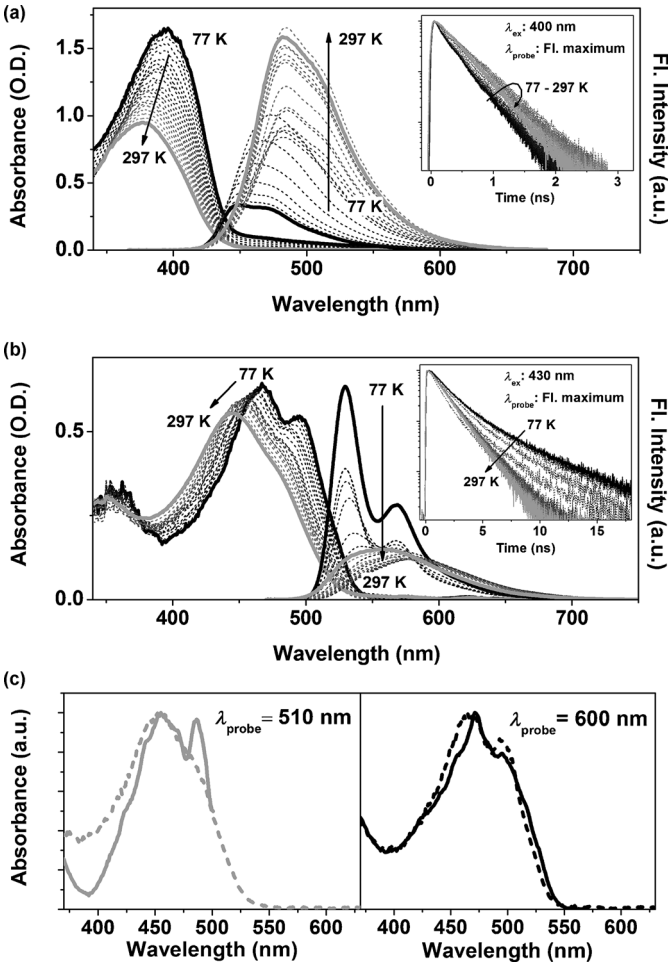

Figure 2. Temperature-dependent steady-state absorption and fluorescence spectra of a) compound **S3** and b) compound **S6** in 2-methyltetrahydrofuran (mTHF) from 77 K to 297 K. c) Fluorescence excitation spectra (solid lines) of compound **S6** at 77 K, probed at 510 and 600 nm, and their corresponding absorption spectra (dotted lines), collected at 217 and 77 K, respectively.

Numerous works on oligothiophenes have reported that their broad absorption spectra are the consequence of superposition of absorption bands of various non-planar conformers with small energy differences ($\Delta E < k_B T$). In contrast, in the excited state, non-planar conformers undergo geometrical relaxation, a so called "planarization process", toward a planar conformation with a quinoid-like structure.[29,31,32] Many investigations on the energy-relaxation dynamics of linear oligothiophenes have been reported, but studies on dendrimer-type structures are still in an early stage because of their structural complexity. In general, dendrimer-type oligothiophenes are more rigid compared to linear ones, owing to their bulky structure. The large Stokes shift indi-

cates that the molecular geometries between the ground- and excited-state are largely different. Herein, the Stokes shift of compound **S3** is larger than that of compound **S6** because the geometrical relaxation of compound **S6** is suppressed by the overcrowded 24 butyl groups. This suggestion enables us to explain their photophysical properties: First, a relatively slow torsional relaxation time (25 ps) of compound **S6** compared to that of compound **S3** (14 ps) was obtained from the femtosecond transient absorption (fs-TA) measurements. Second, any distinct spectroscopic shifts were not shown in the fs-TA spectra of compound **S6**, whereas those of compound **S3** exhibited a red-shift in the TA spectra as a function of time (see the Supporting Information, Figure S4). Finally, the fluorescence intensity of compound **S6** decreased as the temperature increased, which was an opposite trend to that of compound **S3**. As a consequence, although the photoinduced reorientation of compound **S6** undergoes a planarization process, this process might not be as effective as in compound **S3**. In this regard, we not only focused on the π-conjugation length but also on the molecular rigidity to understand the energy-relaxation processes of compounds **S3** and **S6**.

At 77 K, the ground-state structures of compounds **S3** and **S6** deviate from the planarity on account of the butyl substituents on the thiophene rings. Compared to these structures at low temperatures, at room temperature, compounds **S3** and **S6** have largely twisted structures because thermally activated out-of-plane bending motions of the thiophene rings allow an increase in the torsion angles.[26,33] Figure 2a,b shows that, on increasing the temperature, the absorption spectra of compounds **S3** and **S6** are gradually blue-shifted because the π-electron delocalization along the conjugated backbone is disruptive in the twisted structure. However, the fluorescence spectra of compounds **S3** and **S6** are red-shifted on increasing the temperature from 77 to 217 K, owing to a planarization process in the excited-state.

Intriguingly, the fluorescence spectra of compounds **S3** and **S6** show opposite trends in the intensity change with increasing temperature. As the temperature increases, the fluorescence intensity of compound **S3** increases and its fluorescence lifetime becomes longer. In contrast, the fluorescence intensity of compound **S6** exhibits a maximum value at 77 K and then decreases with increasing temperature. In addition, the fluorescence-decay profile shows bi-exponential decay at low temperatures; however, it becomes mono-exponential decay at room temperature. The resultant ratios between the long (3.0 ns) and short lifetime components (1.3 ns) in the fluorescence-decay profiles of compound **S6** at various temperatures (77–297 K) are summarized in Table 2. At low temperatures, the fluorescence lifetime of 1.3 ns occupies 58.1 % of all of the decay processes and accounts for 93.5 % at room temperature. On the basis of these observations, to understand the increase in fluorescence intensity of compound **S3** with increasing temperature, we calculated radiative and nonradiative decay rates. The nonradiative decay rates have been categorized as two processes, internal conversion and intersystem crossing. Because the number of vibrational modes of the molecule and the number of phonons to be activated are larger at room temperature than at low temperatures, the rate of nonradiative decay commonly increases with increasing temperature. However, in this study, the nonradiative decay rate decreases, although the radiative decay rate remains almost constant with increasing temperature (Table 2). This result shows that the nonradiative decay rate of compound **S3** is mainly determined by an intersystem crossing (ISC) process. The change in fluorescence lifetime with temperature is discussed in more detail with respect to the ISC transition below, along with the energy-relaxation process. The fluorescence intensities of compound **S6** decrease because the number of thermally activated vibrational modes increase with increasing temperature and the fluorescence lifetime of compound **S6** (1.3–3.0 ns) is much longer than that of directly linked six-ring linear oligothiophenes (about 700 ps).[28] In this regard, we can suggest that the molecular rigidity of compound **S6** has a considerable effect on its fluorescence lifetime.

Table 2. Fluorescence lifetimes of compounds **S3** and **S6** at various temperatures.

T [K]	**S3**			**S6**	
	τ_F [ps]	k_r [$\times 10^8$ s^{-1}]	k_{nr} [$\times 10^8$ s^{-1}]	τ_F [%]	
				1.3 ns	3 ns
77	233	8.58	34.3	58.1	41.9
127	255	9.80	29.4	73.5	26.5
207	402	7.96	16.9	89.9	10.1
257	380	9.21	17.1	90.2	9.8
297	338	9.46	20.1	93.5	6.5

Based on their calculated optimized structures, we suggested that the different conformers of compounds **S3** and **S6** coexisted with energy differences between the conformers. To obtain clear evidence to support this suggestion, we analyzed the fluorescence excitation spectra of compounds **S3** and **S6** at 77 K, as probed at the blue- and red-edge regions for each molecule (Figure 2c). Whilst there is no distinguishable difference between the two fluorescence excitation spectra of compound **S3**, the ground-state molecular structures of compound **S6** at 77 K can be readily determined by comparing the fluorescence excitation spectra with the absorption spectra. The fluorescence excitation spectra at the blue- and red-edge regions of the emission agree well with the absorption spectra at 217 and 77 K, respectively. This result shows that compound **S6** adopts two conformers that show distinctive geometrical differences in the ground state, that is, "planar" and "twist" conformers, with a large energy barrier between them. Because the molecular backbone of compound **S6** is more twisted at 217 K than at low temperatures and because the proportion of the fast decay component (1.3 ns) gradually increases as the temperature increases, we expect that the short fluorescence lifetime (1.3 ns) originates from the relatively twisted structure. Because the spectroscopic observation is based on the emitting units, the "planar" and "twist" notations are attributed to the torsional angles within each chromophore for

compound **S6**. These "planar" and "twist" structures agree well with optimized structures **S6A** and **S6B**, respectively. In this respect, more-convincing evidence was obtained, as discussed below.

Single-molecule spectroscopy: The coexistence of different conformers in the system with six terthiophene arms has been revealed by using temperature-dependent spectroscopic techniques, although the geometries of these conformers were not clarified. Furthermore, in the three arm system, the conformational differences were not observed by the spectroscopic method due to the structural flexibility. Ensemble measurements are essential in the investigation of molecular properties, but they often preclude detailed information at the single-molecule level by averaging over all the measured observables. As a consequence, the ensemble properties are likely to conceal unique contributions from each conformer of compounds **S3** and **S6**. On account of this result, we measured the single-molecule fluorescence intensity trajectories and fluorescence lifetimes by using single-molecule fluorescence microscopy. The fluorescence intensity trajectories (FITs) of compounds **S3** and **S6**, which correspond to the changes in fluorescence intensity of each single molecule as a function of time, have been recorded upon photoexcitation at wavelengths of 405 and 450 nm, respectively.

The relative proportions of the number of intensity steps in the FITs are listed in Table 3. Four representative FITs of 149 single molecules of compound **S3** and 159 single molecules of compound **S6** are shown in Figure 3 and Figure 5, respectively. Approximately 69% of the molecules of compound **S3** exhibit three-step photobleaching behavior, in accordance with the number of constituent terthiophene units. On the other hand, more than 95% of the molecules of compound **S6** show a smaller number of emissive levels than the number of arms and even exhibit much-simpler behaviors in their FITs than compound **S3**.

Table 3. Ratio of the number of intensity steps in the FITs for compounds **S3** and **S6**.

	1 Step		2 Steps		3 Steps		Multistep	
S3	7/149	4.6%	39/149	26.3%	103/149	69.1%	–	–
S6	79/159	49.7%	51/159	32.1%	22/159	13.8%	7/159	4.4%

For molecules of compound **S3**, if the FITs show the same number of steps as the number of terthiophene units, simultaneous analysis of the FITs and fluorescence lifetimes would allow an observation of the photobleaching dynamics, based on the photobleaching sequence of individual chromophores. Furthermore, as shown in Figure 3, the photobleaching dynamics of compound **S3** can be classified into two representative cases, according to whether the long fluorescence lifetime (about 1.4 ns) is observed or not. It is noteworthy that a long fluorescence lifetime, as with compound **S6**, is also observed for compound **S3**. In a particular structure, this feature probably arises from the two electronically communicating terthiophene arms. As shown in Scheme 1a, two different conformations, namely **S3A** and **S3B**, have been investigated by computing their optimized structures. In accordance with this supposition, almost half of the cases show similar fluorescence lifetimes (about 400 ps) at both the first and second emissive levels among the three-step intensity levels in compound **S3** (Figure 3a). This feature is attributable to the three electronically non-interacting thiophene arms in compound **S3A**, which separately emit fluorescence. On the other hand, the remaining cases, which exhibit a long fluorescence lifetime (about 1.4 ns), can be categorized into three different subcases according to the characteristics of the first and second emissive levels in the FITs. Based on the observed fluorescence lifetimes of compounds **S3** and **S6** in solution (Figure 1b), the long fluorescence lifetime is ascribed to the electronically interacting terthiophene arms. It is known that the molecular linearity can induce better conjugation in organic molecules. In this respect, it is conceivable that the long fluorescence lifetime is observed in structure **S3B** because of its enhanced linearity between the two terthiophene arms compared to structure **S3A**. For simplicity, we refer to the terthiophene units in structure **S3B** as t1–t3, starting from the left in a clockwise turn, and we assume that unit t2 may electronically interact with unit t3.

In Figure 3b, the fluorescence lifetime of the first emissive level is three-times longer than those of the second and third levels and the respective fluorescence lifetimes are 1.39 ns, 380 ps, and 420 ps, respectively. It is thought that the molecule exhibits further augmentation in exciton delocalization at the first level, which can occur if the molecule follows the photobleaching sequence: unit t3 (or t2)→t2 (or t3)→t1 (Figure 3b); on the other hand, the first and second levels of the FIT in Figure 3c show long fluorescence lifetimes. We attribute this feature to the photobleaching sequence: t1→t2 (or t3)→t3 (or t2). Herein, the first emissive level exhibits a similar fluorescence lifetime compared to the second level, with higher intensity because of the difference between the fluorescence efficiencies of delocalized and localized excitons in the molecule. Although one of the terthiophene units photobleaches first, the molecule still maintains the delocalized exciton along the *meta* linker at the second emissive level. In the last case, the FIT in Figure 3d shows that the fluorescence lifetime of the first level is three-times shorter than that of the second level. In this case, the molecule might follow the photobleaching sequence: t1→t2 (or t3)→t3 (or t2), as shown in Figure 3c. However, a striking difference is observed in the first emissive level. In Figure 3d, there is no electronic communication between units t2 and t3 in the first level, owing to geometrical reasons.

To explain the change in fluorescence lifetime between the first and second emissive levels, molecular planarity was also taken into consideration. In the expected structure of conformer **S3B**, the innermost thiophene ring of one conjugated thiophene arm is almost orthogonally attached to the

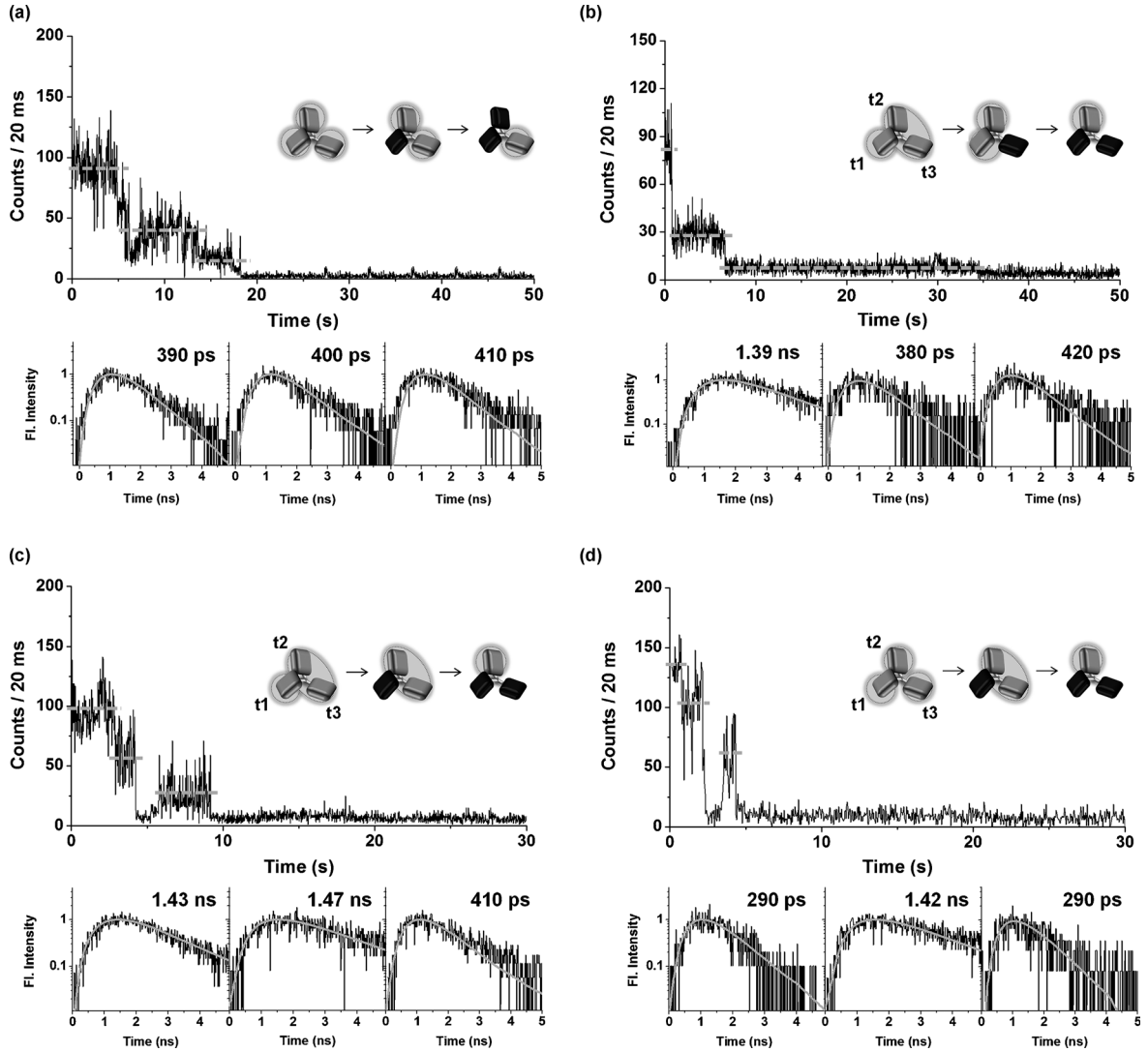

Figure 3. Representative fluorescence-intensity trajectories (FITs) and fluorescence-decay profiles of structures a) **S3A** and b)–d) **S3B**, which correspond to each emissive level after photoexcitation at 405 nm. Two conformations of the star-shaped oligothiophene trimer, that is, **S3A** and **S3B**, coexist in solution.

plane of the phenyl core, whilst the other innermost thiophene rings of two arms are in the same plane as the core. In this conformation, the electronic communication between the two arms along the *meta* linker is non-negligible. However, after the electronic interaction along the *meta* linker is interrupted by increasing the dihedral angle between the core and the adjacent thiophene ring, two terthiophene arms separately emit fluorescence. It is likely that the long fluorescence lifetimes, whether they are shown in the first emissive level or not, stem from a conformational change in the innermost thiophene ring by repeated excitation. Owing to low torsional barriers in the excited state ($<k_BT$), the conformational change in structure **S3B** can be induced by thermal energy, which results from repeated excitation laser pulses.[34–36] In accordance with these results, the constructed fluorescence-lifetime distributions of compound **S3**, with the fitted fluorescence lifetime at the first and second emissive levels, show bimodal features, as shown in Figure 4a. The distributions are fitted by two Gaussian functions with mean values of 410 ps and 1.41 ns. The long fluorescence lifetimes are mainly shown at the first emissive level. In contrast, the number of events to show short lifetimes at the second emissive level increases, because electronic communication along the *meta* linker is easily broken and, hence, it is harder to move the two arms into the same plane than to change the dihedral angle of one arm.

Based on the fact that the exciton is spatially located in the *para*-arranged terthiophene arms, the number of chromophores in compound **S6** is three. Thus, an expected FIT for compound **S6** should have three emissive levels. However, almost half of the molecules of compound **S6** exhibit one-step photobleaching behavior and 32% of the molecules exhibit two-step photobleaching in FITs (Figure 5a,b). As shown in Figure 5, the FIT with a single intensity level

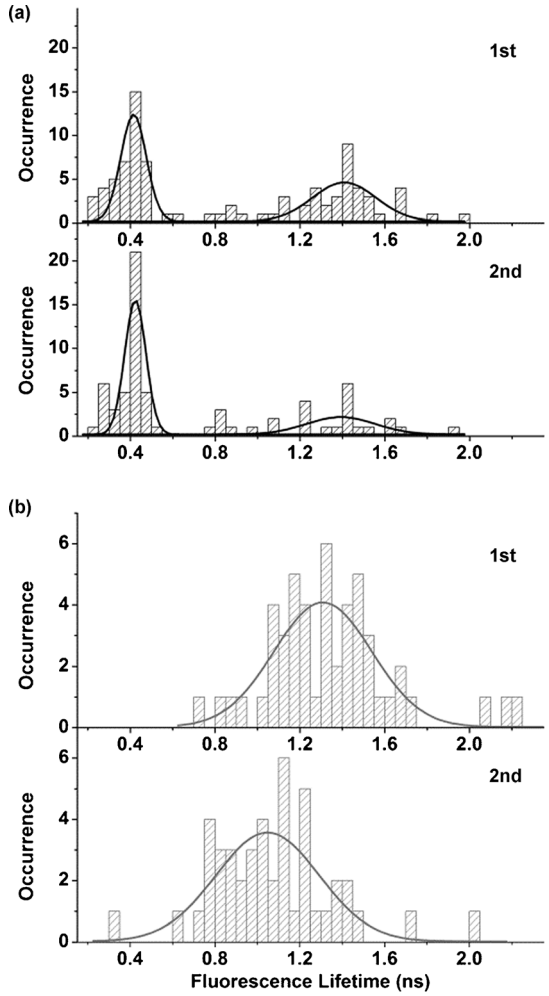

Figure 4. Fluorescence-lifetime distributions of a) compound **S3**, which shows three-step photobleaching behavior, and b) compound **S6**, which shows one- and two-step photobleaching behavior. The fluorescence lifetimes of single molecules were determined in the first (top) and second emissive levels (bottom). The histograms were constructed by collecting more than a) 100 and b) 50 single-molecule datasets for each molecule. The solid lines correspond to fitted Gaussian curves. The third emissive level of compound **S3** is excluded from the fluorescence-lifetime distributions because a number of third steps show too-low fluorescence intensity for a reliable fitting of the data.

shows the longest fluorescence lifetime (1.52 ns) compared to those with two intensity levels, in which the first emissive level shows a longer fluorescence lifetime of 1.31 ns than that of the second emissive level. It is noteworthy that the mean fluorescence lifetime of the second emissive level (1.05 ns) is more than two-times longer than that of compound **S3** (about 400 ps). This result indicates that the emitting unit for the second emissive level is not on the single terthiophene arm. In accordance with these above results, the constructed fluorescence-lifetime distribution of molecules of compound **S6**, which show two-step photobleaching behavior as a decrease in the central value on going from its first to second intensity levels (Figure 4b).

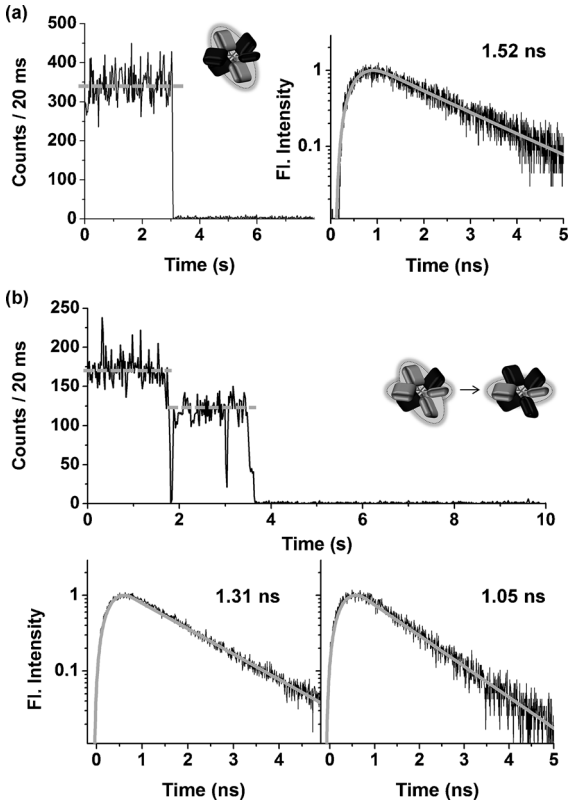

Figure 5. Representative fluorescence-intensity trajectories (FITs) and fluorescence-decay profiles of structures a) **S6A** and b) **S6B**, which correspond to each emissive level after photoexcitation at 450 nm.

A previous study on thiophene dendrimer systems found that arms with small dihedral angles were expected to have better π conjugation with the core compared to those with large dihedral angles based on the optimized ground- and excited-state structures.[33] In the same manner, the optimized ground-state structure of compound **S6A** has largely different dihedral angles between the core and each of the adjacent thiophene rings (84.4, 2.4, 77.1, 65.2, 8.2, and 28.8°). Thus, in structure **S6A**, we expect that the π conjugation is solely elongated along the arms with dihedral angles of 8.2 and 2.4° (*para* to each other). However, the two-step photobleaching dynamics of compound **S6** account for almost 30% of the molecules. This feature can corroborate the presence of a different conformer, **S6B**, in which two of the three *para*-positioned arms have small dihedral angles. The neighboring innermost thiophene rings, in which the two sulfur atoms face each other, and their *para*-positioned counterparts form relatively smaller dihedral angles compared to the rest (see the Supporting Information, Figure S1). The shorter fluorescence lifetime in the second emissive level compared to that in the first emissive level can be elucidated by the differences between the dihedral angles on two *para*-arranged arms. In the first emissive level, two *para*-positioned arms are excited. However, the longest chromophore with enhanced conjugation length, which has a smaller dihedral angle, emits fluorescence first

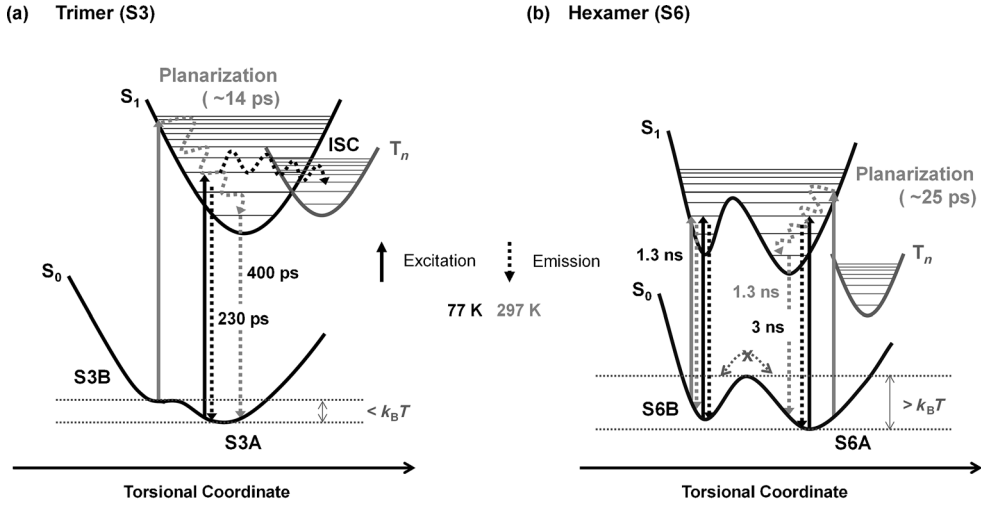

Figure 6. Energy-relaxation diagrams of compounds **S3** and **S6**. Schematic representation of energy relaxation for a) **S3** and b) **S6**, based on the torsional angles within each chromophore. The ground-state structures at various temperatures are deviated from planarity, owing to the butyl substituent; however, the planarization process accompanies a geometrical change, which allows neighboring thiophene rings to form quinoid-like structures.

and, after a photobleaching event, a second emission. Herein, a decrease in the intensity level was observed owing to the decreased absorption capability by photobleaching event. These features explain that electronic communication through the core structure is highly sensitive to the dihedral angle between the core structure and the arms in large star-shaped oligothiophenes.

Energy-relaxation processes: On the basis of a combination of spectroscopic measurements and quantum chemical calculations, a schematic representation of energy-relaxation processes in compounds **S3** and **S6** was conceived (Figure 6). The excited-state processes, including vibronic relaxation, fluorescence, and ISC, which take place upon photoexcitation (solid arrows), are denoted by dotted arrows.

Previous work on directly linked linear oligothiophenes verified that an overlap integral between the vibrational wave packets in the singlet and triplet states was influenced by the chain length and the torsional angles between the thiophene rings.[30,37,38] Both parameters, that is, thiophene chain length and torsional angles, play decisive roles in determining the π-conjugation length in these systems. Previous studies on directly linked linear oligothiophenes, along with the radiation-less transition rates within the temperature range 77–297 K (as a part of this study), enable us to postulate that the fluorescence lifetime for compound **S3** is mainly determined by the ISC transition.

We calculated the vertical transition energies from the S_0 to S_1 states, as well as the energy difference between the S_0 and T_n states of both twisted and planar structures for compound **S3** by considering the planarization process in the excited state.[38] At this stage, it is worth noting that the all-*meta* arrangements of terthiophene arms around a phenyl core result in photophysical properties that are dominated by a single terthiophene arm. In this manner, for compound **S3**, we postulate that the photoinduced planarization process is limited to the single terthiophene arm. At 77 K, the structure of conformer **S3A** in the excited state is the same as that in the twisted ground-state structure because the planarization process is hampered by the frozen matrix. At low temperatures, only conformer **S3A** is conceivable because it has a lower potential energy compared to conformer **S3B**. On the other hand, at room temperature, the photoexcited terthiophene arm induces the planarization process and the conformation of compound **S3** becomes planar in the excited state. The effective π-conjugation length is elongated after planarization. Because the ISC process is not spin-allowed, the planarization process is much faster than the ISC process. On account of the elongated π-conjugation length, the fluorescence lifetime becomes longer with a dramatic decrease in the nonradiative rate as the temperature increases. According to the calculations, the T_n state of the twisted structure is located below the S_1 state; however, that of the planar structure is located in the vicinity of the S_1 state (see the Supporting Information, Figure S5). From these quantum mechanical calculations and the experimental observations, we can clearly demonstrate that the ISC rate largely decreases after the planarization process because an overlap integral between the single and triplet states is directly related to the ISC rate (k_{isc}). In contrast with single-molecule spectroscopic measurements, the long fluorescence lifetime for structure **S3B** is not likely to be observable in the solution phase, owing to its shallow potential-energy curve.

Moreover, as shown in Figure 6b, the overcrowded 24 butyl groups in compound **S6** are likely to result in a high potential barrier between the two different conformers ($>k_BT$), that is, **S6A** and **S6B**, in the ground state. By lowering the temperature, we can distinguish between the conformers of compound **S6** by using spectroscopic methods: At 77 K, two distinguishable fluorescence lifetimes (1.3 and 3.0 ns) were observed. However, upon increasing the tem-

perature, the bi-exponential fluorescence-decay profile gradually changed into a mono-exponential one, with a long lifetime of 3.0 ns. As described above, an increase in the π-conjugation length of substituted oligothiophenes, which is mainly determined by the dihedral angle between the thiophene rings, slows the rate of ISC. In this respect, we suggest that the long fluorescence lifetime (3.0 ns) originates from the conformation of structure **S6A**, in which the π electrons are highly delocalized because of the smaller dihedral angle between the neighboring thiophene rings than in structure **S6B**. On the other hand, the short fluorescence lifetime (1.3 ns) is attributable to structure **S6B**, in which the two facing innermost thiophene rings force adjacent thiophene ring to maintain a large dihedral angle.

Now, the question of how the mono-exponential decay profile for compound **S6** was observed at room temperature remains, despite the high potential barrier between the two conformers. This question can be answered by comparing the structural rigidity of structures **S6A** and **S6B**. As the temperature increases, the long fluorescence lifetime of structure **S6A** at low temperatures becomes shorter because a number of vibrational modes of structure **S6A** are activated at room temperature. This feature agreed well with the planarization process (about 25 ps), which was observed by performing fs-TA measurements. However, in the case of structure **S6B**, steric congestion between the butyl groups that are attached onto the two facing terthiophene arms hampers geometrical relaxation processes and the fluorescence lifetime is likely to be independent of temperature. Accordingly, although two distinctive fluorescence lifetimes were observed at 77 K, only a short fluorescence lifetime of about 1.3 ns was obtained at room temperature, despite the fact that its fluorescence originated from the two different conformers.

Conclusion

The connection of terthiophene arms onto either the *meta* or *para* positions of an ethynylbenzene core has been envisaged from a theoretical perspective to comparatively investigate electronically interacting and non-interacting systems. In this study, we have elucidated the structure-dependent interchromophoric interactions and the energy-relaxation processes in compounds **S3** and **S6** by analyzing their fluorescence-lifetime distributions at the single-molecule level, as well as their changes in fluorescence lifetimes and spectroscopic peak-shifts with increasing temperature at the ensemble level. Notably, we revealed the existence of not only strong electronic communication between the substituent arms for compound **S6**, but also weak communication for compound **S3** by performing single-molecule spectroscopic measurements, which were difficult to observe by performing ensemble measurements. For example, delocalized π electrons along the *meta* linker and a corresponding long-fluorescence lifetime of about 1.4 ns have been observed at the single-molecule level. Based on these observations, we identified that the electronic interactions largely were correlated with the molecular conformations of compounds **S3** and **S6**. The electronic interactions are significantly affected by the dihedral angle between the phenyl core and each terthiophene arm, as well as by the substituted position. Consequently, the comparative studies on compounds **S3** and **S6**, in terms of their molecular structures and interactions between the constituent units, provide important information for understanding the contrasting fluorescence properties of these two molecular systems, in which thiophene arms are linked at three different positions, that is, *ortho*, *meta*, and *para* substitution. Thus, the relationship between the molecular structures and photophysical properties of molecular arrays of different shapes can guide our design of molecular assemblies for promising applications as effective electronic/photonic devices.

Experimental Section

Sample preparation: A detailed description of the synthesis of compounds **S3** and **S6** was reported in a previous paper.[22] Samples for single-molecule spectroscopic measurements were prepared by spin-coating (2000 rpm) solutions of the star-shaped oligothiophenes ($\times 10^{-10}$ M) in toluene (anhydrous, ≥99.9%, spectrophotometric grade, Aldrich) that contained 10 mg mL^{-1} poly(methylmethacrylate) (PMMA) onto thoroughly cleaned quartz coverslips and glass coverslips. All of the glassware that were used for the sample preparation were cleaned by sonication in acetone, an aqueous solution of NaOH (10%), and Milli-Q water.

Single-molecule spectroscopy: A confocal microscope system, based on an inverted-type microscope that was coupled to a picosecond-pulsed 405 nm and 450 nm diode laser (10 MHz repetition rate, pulse width <90 ps, PicoQuant), was employed to detect the fluorescence of single molecules. The collimated laser beam was sent to a wave plate to ensure circularly polarized light and then delivered to the input port of a confocal microscope after passing through a beam expander to ensure a large enough beam size at the back focal plane. Then, the laser beam was reflected by using a dichroic mirror and focused onto the sample through an oil-immersion objective lens (×100, numerical aperture = 1.3, Nikon). Fluorescence emission was collected by using the same objective lens, passed through a dichroic mirror, cleaned with a notch filter and longpass filters, and focused through a lens (focal length: 100 mm) into an active area of an avalanche photodiode (APD; SPCM-AQR-16-FC, EG&G, Perkin–Elmer Optoelectronics). The sample positions were controlled by using a piezoelectric tube scanner (XE-120, Parksystem). The signal from the APD was delivered into a TCSPC card (SPC-830, Becker and Hickl GmbH) that was operated in FIFO (first-in-first-out) mode, which could construct the fluorescence-intensity trajectory with a specific bin time and fluorescence-decay profiles with an experimental instrument response of 500 ps. We convoluted the fitting function with the response function to arrive at the early time rise, as displayed by the fits. The maximum likelihood estimation (MLE) was used to fit the fluorescence decays. Maus et al. demonstrated that, because the MLE method was based on more-adequate multinomial statistics, it could provide a precise fluorescence-lifetime determination for a few photons in single-molecule fluorescence. In that paper, the LS (least-squares) and MLE methods were experimentally compared and, from the distribution of the fitted lifetimes against the number of counts per decay, it was found that the lifetimes as estimated by using the MLE method were 5% larger than those estimated by using the LS method.[39] A detailed description of the setup and the data-acquisition process have been published previously.[40] We defined the fluorescence lifetimes of the solid bulk film as the lifetime of the fluorescence decay that was made up from the data of all of the pixels of a scanned area.

Ensemble spectroscopy: Steady-state absorption spectra were recorded on a UV/Vis spectrometer (Cary5000, Varian) and emission spectra were recorded on a fluorometer (F-2500, Hitachi). Fluorescence quantum yields were determined in toluene and compared with that of a rhodamine 6G standard in EtOH (0.95) as a reference at an excitation wavelength of 480 nm. Time-resolved fluorescence spectra were recorded by using a time-correlated single-photon-counting (TCSPC) technique. As an excitation light source, we used a homebuilt cavity-dumped Ti:sapphire oscillator, which provided a high repetition rate (200–400 kHz) of ultrashort pulses (100 fs at full-width-at-half-maximum (FWHM)), pumped by a continuous wave (CW) Nd:YVO4 laser (Verdi, Coherent). The output pulses of the oscillator were frequency doubled with a second harmonic BBO crystal. The FWHM of the instrument-response function (IRF), as obtained for a dilute solution of coffee cream, was typically 30 ps in our TCSPC system. For all temperature-dependent measurements, a temperature-controlled liquid-nitrogen cryostat (Oxford Instruments, Optistat DN) was used. Temperatures were maintained within ± 0.05 K and allowed to equilibrate for at least 10 min before each scan.

Acknowledgements

The work at Yonsei University was financially supported by the Mid-Career Researcher Program (2010-0029668), the Global Frontier R&D Program of the Center for Multiscale Energy System (2012-8-2081), and the World Class University Program (R32-2012-000-10217-0) of the 10 National Research Foundation (NRF), funded by the Ministry of Education, Science and Technology (MEST) of Korea. The work at Tokyo Metropolitan University was supported by a Grant-in-Aid for Scientific Research from the Japan Society for the Promotion of Science (JSPS) and by the Japan Science and Technology (JST). The authors thank Prof. W. Fujita (Tokyo Metropolitan University) for performing the X-ray analysis of hexakis(5-hexyl-2-thenylethynyl)benzene.

[1] M. A. Green, K. Emery, Y. Hishikawa, W. Warta, *Prog. Photovoltaics* **2010**, *18*, 346–352.
[2] J. Shinar, R. Shinar, *J. Phys. D* **2008**, *41*, 133001–133026.
[3] S. Reineke, F. Lindner, G. Schwartz, N. Seidler, K. Walzer, B. Luessem, K. Leo, *Nature* **2009**, *459*, 234–238.
[4] S. Lo, P. L. Burn, *Chem. Rev.* **2007**, *107*, 1097–1116.
[5] F. Garnier, G. Horowitz, D. Fichou, *Synth. Met.* **1989**, *28*, 705–714.
[6] A. Mishra, C. Ma, P. Bäuerle, *Chem. Rev.* **2009**, *109*, 1141–1276.
[7] T. Goodson, *Annu. Rev. Phys. Chem.* **2005**, *56*, 581–603.
[8] D. Astruc, E. Boisselier, C. Ornelas, *Chem. Rev.* **2010**, *110*, 1857–1959.
[9] *Electronic Materials: The Oligomer Approach* (Eds.: K. Müllen, G. Wegner), Wiley-VCH, Weinheim, **1998**.
[10] C. He, Q. He, Y. Yi, G. Wu, F. Bai, Z. Shuai, Y. Li, *J. Mater. Chem.* **2008**, *18*, 4085–4090.
[11] M. K. R. Fischer, C. Q. Ma, R. A. J. Janssen, T. Debaerdemaeker, P. Bäuerle, *J. Mater. Chem.* **2009**, *19*, 4784–4795.
[12] C. Q. Ma, M. Fonrodona, M. C. Schikora, M. M. Wienk, R. A. J. Janssen, P. Bäuerle, *Adv. Funct. Mater.* **2008**, *18*, 3323–3331.
[13] N. Kopidakis, W. J. Mitchell, J. v. d. Lagemaat, D. S. Ginley, G. Rumbles, S. E. Shaheen, W. L. Rance, *Appl. Phys. Lett.* **2006**, *89*, 103524.
[14] T. W. Lee, D. C. Kim, N. S. Kang, J. W. Yi, M. J. Cho, K. H. Kim, D. H. Choi, *Chem. Lett.* **2008**, *37*, 866–867.
[15] Y. G. Kim, H. Christian-Pandya, N. Ananthakrishnan, Z. I. Niazimbetova, B. C. Thompson, M. E. Galvin, J. R. Reynolds, *Sol. Energy Mater. Sol. Cells* **2008**, *92*, 307–312.
[16] C. J. Xia, X. W. Fan, J. Locklin, R. C. Advincula, A. Gies, W. Nonidez, *J. Am. Chem. Soc.* **2004**, *126*, 8735–8743.
[17] S. A. Ponomarenko, S. Kirchmeyer, A. Elschner, B. H. Huisman, A. Karbach, D. Drechsler, *Adv. Funct. Mater.* **2003**, *13*, 591–596.
[18] W. J. Mitchell, N. Kopidakis, G. Rumbles, D. S. Ginley, S. E. Shaheen, *J. Mater. Chem.* **2005**, *15*, 4518–4528.
[19] C. Q. Ma, E. Mena-Osteritz, T. Debaerdemaeker, M. M. Wienk, R. A. J. Janssen, P. Bäuerle, *Angew. Chem.* **2007**, *119*, 1709–1713; *Angew. Chem. Int. Ed.* **2007**, *46*, 1679–1683.
[20] R. D. McCullough, *Adv. Mater.* **1998**, *10*, 93–116.
[21] C. J. Xia, X. W. Fan, J. Locklin, R. C. Advincula, *Org. Lett.* **2002**, *4*, 2067–2070.
[22] T. Narita, M. Takase, T. Nishinaga, M. Iyoda, K. Kamada, K. Ohta, *Chem. Eur. J.* **2010**, *16*, 12108–12113.
[23] T. M. Pappenfus, K. R. Mann, *Org. Lett.* **2002**, *4*, 3043–3046.
[24] M. Hasegawa, J. Takano, H. Enozawa, Y. Kuwatani, M. Iyoda, *Tetrahedron Lett.* **2004**, *45*, 4109–4112.
[25] N. DiCésare, M. Belletête, A. Donat-Bouillud, M. Leclerc, G. Durocher, *Macromolecules* **1998**, *31*, 6289–6296.
[26] N. DiCésare, M. Belletête, M. Leclerc, G. Durocher, *Chem. Phys. Lett.* **1998**, *291*, 487–495.
[27] W. J. Mitchell, A. J. Ferguson, M. E. Köse, B. L. Rupert, D. S. Ginley, G. Rumbles, S. E. Shaheen, N. Kopidakis, *Chem. Mater.* **2009**, *21*, 287–297.
[28] R. S. Becker, J. Seixas de Melo, L. A. Maçanita, F. Elisei, *J. Phys. Chem.* **1996**, *100*, 18683–18695.
[29] S. Cho, M. Yoon, C. H. Kim, N. Aratani, G. Mori, J. Taiha, A. Osuka, D. Kim, *J. Phys. Chem. C* **2007**, *111*, 14881–14888.
[30] D. Beljonne, Z. Shuai, G. Pourtois, J. L. Bredas, *J. Phys. Chem. A* **2001**, *105*, 3899–3907.
[31] F. J. Ramírez, M. A. G. Aranda, V. Hernández, J. Casado, S. Hotta, J. T. López Navarrete, *J. Chem. Phys.* **1998**, *109*, 1920–1929.
[32] S. Westenhoff, W. J. D. Beenken, R. H. Friend, N. C. Greenham, A. Yartsev, V. Sundström, *Phys. Rev. Lett.* **2006**, *97*, 166804.
[33] M. E. Köse, W. J. Mitchell, N. Kopidaks, C. H. Chang, S. E. Shanheen, K. Kim, G. Rumbles, *J. Am. Chem. Soc.* **2007**, *129*, 14257–14270.
[34] J. Sjöqvist, M. Linares, M. Lindgren, P. Norman, *Phys. Chem. Chem. Phys.* **2011**, *13*, 17532–17542.
[35] M. Breza, V. Lukes, I. Vrabel, *J. Mol. Struct. THEOCHEM* **2001**, *572*, 151–160.
[36] S. S. Zade, M. Bendikov, *Chem. Eur. J.* **2007**, *13*, 3688–3700.
[37] D. Beljonne, J. Cornil, R. H. Friend, R. A. Janssen, J. L. Brédas, *J. Am. Chem. Soc.* **1996**, *118*, 6453–6461.
[38] E. Badaeva, M. R. Harpham, R. Guda, O. Süzer, C. Q. Ma, P. Bäuerle, T. Goodson, S. Tretiak, *J. Phys. Chem. B* **2010**, *114*, 15808–15817.
[39] M. Maus, M. Cotlet, J. Hofkens, T. Gensch, F. C. De Schryver, J. Schaffer, C. A. M. Seidel, *Anal. Chem.* **2001**, *73*, 2078–2086.
[40] T. Vosch, M. Cotlet, J. Hofkens, K. Van der Biest, M. Lor, K. Weston, P. Tinnefeld, M. Sauer, L. Latterini, K. Müllen, F. C. De Schryver, *J. Phys. Chem. A* **2003**, *107*, 6920–6931.

Received: January 28, 2013
Published online: June 4, 2013

